Segregation induced by phase synchronization in a bidisperse granular layer

Tai-Yuan Wang and T. M. Hong
Department of Physics, National Tsing Hua University, Hsinchu 30043, Taiwan, Republic of China
(Received 18 May 2008; revised manuscript received 30 August 2008; published 16 December 2008)

We propose an alternative segregation mechanism where the species-dependent interactions are dynamically induced by the phase synchronization of beads. Based on this scenario, we report an alternative segregation among beads of different restitution coefficients by molecular dynamics simulations. Since the beads are of equal size and mass, this is not related to the Brazilian-nut effect, nor can it be explained by the depletion force. Instead, this phenomenon derives from the phase synchronization, a concept which helps us determine the criteria for segregation and the phase boundaries that agree excellently with the simulation results.

DOI: 10.1103/PhysRevE.78.061301 PACS number(s): 45.70.−n, 05.70.Fh, 05.70.Ln, 83.10.Rs

Granular material under external vibrations is a nonequilibrium system which is characterized by the competition between external energy input from the vibrating shaker and internal dissipation due to the inelastic collisions. It exhibits many rich and intriguing phenomena, such as pattern formation, segregation, temperature oscillation [1], Maxwell's demon, non-Gaussian velocity distribution, and nonequipartition of energy [2]. Among them, segregation is of particular interest because of its applications in the industry. Mixtures of granular material are known to segregate by size, mass, and friction under different energy inputs, including vertical vibration, horizontal swirling, rotating drum, and other apparatus [3,4]. Several mechanisms have been presented to explain these segregation phenomena, e.g., void filling [5], convection [6], effects of air [7], depletion force [4], or the phenomenological effective potential treatments [8].

In this work, we propose an alternative segregation mechanism where effective interactions are dynamically induced by the phase synchronization of beads. It leads to a horizontal segregation among beads of different restitution coefficients but of equal size and mass. In addition to the event-driven molecular dynamics simulations, we also performed analytic studies to confirm our observation. Since the horizontal Brazilian-nut [3] and the depletion force [4] are no longer applicable, we believe that the concept of phase synchronization is crucial to understand this phenomenon. By analyzing the microscopic trajectories of the vibrated beads, the criteria for the phase synchronization are analytically derived which predict the correct segregation phase diagram from the simulations.

In our model, we confine two species of inelastic spherical granular beads A and B between two horizontal plates on the x-y plane. To exclude the effect of depletion force and other possible segregation mechanisms, their mass and diameter are set to be the same, $m_A=m_B=1$ and $r_A=r_B=1$. However, as will be explained later, our mechanism is not restricted to this requirement. The plates are separated by a fixed distance $h=1.5$ and oscillate vertically along the z direction with trajectories $\Gamma \sin \omega t$ and $h+\Gamma \sin \omega t$, where $\omega=2\pi f$ is the angular frequency and Γ/f denote the amplitude and frequency. The unit of time is chosen in such a way that the gravitational acceleration g pointing in the minus z direction equals 980. The restitution coefficients between plates and beads are $\epsilon_A=0.5$ and $\epsilon_B=0.8$, respectively, and $\epsilon_{AA}=0.5$, $\epsilon_{BB}=0.8$, $\epsilon_{AB}=0.7$ among the beads. The spacing h will be replaced by $H\equiv h-r_A=0.5$ in our calculations, which is a more useful measure of the distance the bead centers can maneuver in the vertical direction. We only present data for the frictionless case because the segregation has been checked to be robust against small slide friction and microscopic roughness on the surface of beads and plates. The way we include the roughness is by assigning Gaussian white noise [9] to the tangential velocity along the plane perpendicular to the normal between colliding beads or between the bead and the plate. The phenomenon has also been checked to be insensitive to the specific choice of parameters used here.

When collisions between beads are rare in the dilute limit, the dynamics of beads can be described separately and the system becomes similar to the inelastic Fermi-Ulam model [10]. Previous studies of this model or the other related bouncer models [11] have shown that under appropriate oscillation conditions there exists a special pattern of motion called the locking phenomenon, where the bead repeats its motion in the z axis and forms a periodic trajectory with a period nT where n is an integer and $T\equiv 1/f$. Here we define a special case of the locking phenomenon named phase synchronization (PS). It requires the trajectory to be both at $n=1$ and behave as a unique stable attractor, into which beads of the same species but different initial conditions will gradually evolve. When PS is established, beads of the same species will automatically synchronize with each other, i.e., their altitude and velocity component in the z axis are the same. Figure 1, obtained by the simulation in the dilute density limit, shows the time evolution of the altitude of beads A under PS. As it demonstrates, the different initial values of altitude and velocity gradually merge into a unique stable trajectory with $n=1$, namely, become synchronized with each other.

In general, PS is not ubiquitous, but only exists for appropriate parameters Γ, f, H, and the bead density. Meanwhile, the shape of the $n=1$ trajectory also depends on the mechanical properties of beads which, thus, prohibit the different species from ever becoming in phase although they can be both in PS (exemplified in Fig. 2). Since the collisions between beads have the potential of disrupting the synchronization, PS is checked to exist only in the submonolayer density, small gap width H, moderate Γ, and sufficiently large f which allow them ample time to return to the $n=1$ trajectory between successive collisions with other beads. The histo-

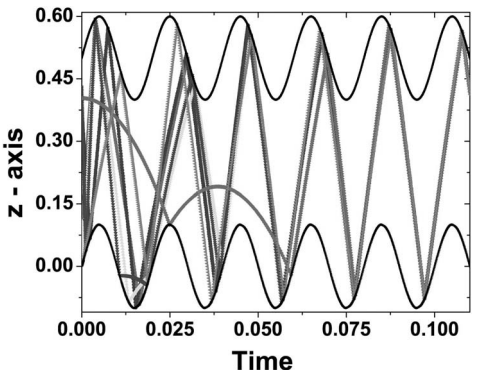

FIG. 1. Spatiotemporal trajectories for beads in the dilute density limit. Here the parameters used are $\Gamma=0.1$ and $f=50$, where PS exists. Beads of different initial altitudes and velocities are represented by separate lines, which gradually evolve into the $n=1$ trajectory and become synchronized.

gram in Fig. 3 depicts the phase of both plates at the instant of collision with bead A under different amplitude Γ. It shows that a single phase or PS is achieved only in a certain window of Γ.

There are two time scales, τ_1 and the mean free time τ_2, in this granular system. The former measures the time it takes for each bead to return to the $n=1$ trajectory after collision, and in general is a function of Γ, f, all ϵ's, and H. When $H=0$, all beads collide with angle $\theta=0$. As H increases, larger collision angle θ becomes possible. This incurs a more severe change of vertical velocities and causes a larger deviation from the $n=1$ trajectory. Consequently, τ_1 is a monotonically increasing function of H. On the other hand, τ_2 is inversely proportional to the bead density. Phase synchronization requires $\tau_1<\tau_2$, and so the maximum choice of H depends on Γ, f, the restitution coefficients, and the bead density. All claims have been confirmed by our simulations.

Inelastic collisions correspond to a restitution coefficient less than unity. However, when we project the collision onto the horizontal x-y plane, the effective restitution coefficient ϵ_{eff}, defined as the ratio of the total horizontal kinetic energy after and before the collision, can be greater than unity. This happens when the momentum is transferred from the z axis to the horizontal directions. The magnitude of ϵ_{eff} depends on the bead velocities, the restitution coefficient and the collision angle θ between the horizontal plane, and the line joining the centers of the colliding beads. In the case $\theta=0$, the collision reduces to the normal type where no momentum is transferred from the vertical direction and ϵ_{eff} is equal to the normal restitution coefficient. For large θ, the energy transfer is more efficient and $\epsilon_{\text{eff}}>1$ is more likely to happen, as is shown schematically in the inset of Fig. 4.

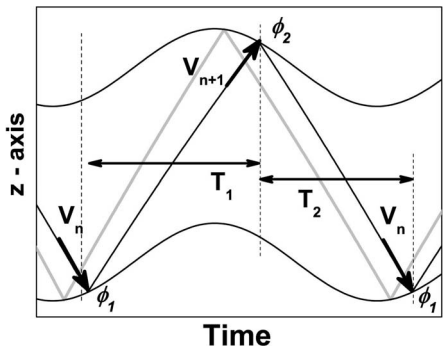

FIG. 2. Trajectories of the two species of beads in PS. Note that A (dark line) and B (gray line) are out of phase. This results in an effective repulsion during their collisions.

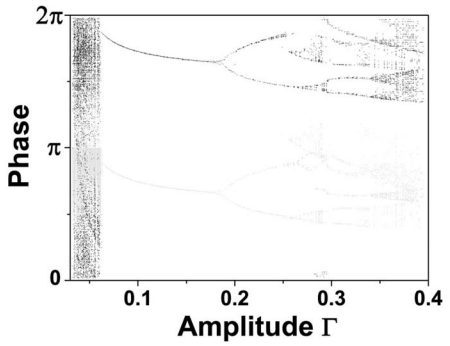

FIG. 3. Simulation results for the phase histogram of bead A upon collisions with the upper and lower plates. Plotted in gray and dark, respectively, they are measured at the instant of collision with bead A against the vibrating amplitude Γ. Phase synchronization or the characteristics of a unique phase is clearly shown to exist only for $0.06<\Gamma<0.18$ approximately.

Beads in PS are synchronized if they belong to the same species; otherwise, they will remain out of phase. Therefore, the θ between A-A (B-B) collisions are mostly zero and their ϵ_{eff} is roughly equal to $\epsilon_{A(B)}$ which is certainly less than unity. Consequently, being out of phase, beads A and B almost always collide at larger θ and result in the $\epsilon_{\text{eff}}>1$ scenario as checked by the simulations and shown in Fig. 4. Hence, upon reaching the PS, collisions of beads between different species are statistically more favorable to gain horizontal kinetic energy and recoil faster, while the same species detach slower because they dissipate more energy in the horizontal directions. These species-dependent interactions lead to the final segregation. Starting from a well mixed initial state, Fig. 5 shows the evolution of the spatial distribution of A (dark area) and B (white area) with the parameters that exhibit PS: $\Gamma=0.1$, $f=50$, and a total of 3136 beads with equal A and B confined in a square box of length 60. Under

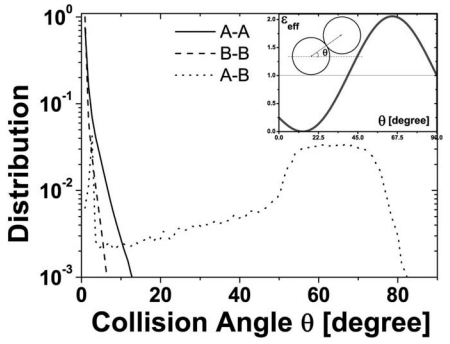

FIG. 4. Simulation results for the distribution of the A-A, B-B, and A-B collision angles during segregation are denoted by the solid, dashed, and dotted lines, respectively. The inset shows the effective restitution coefficient as a function of the collision angle.

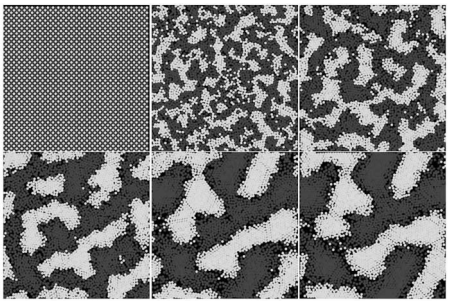

FIG. 5. Projections of bead distribution on the x-y plane show that the spatial patterns develop from mixed to segregated states. The black and white circles represent type-A and -B beads of equal size and mass when $\Gamma=0.1$ and $f=50$. There are totally 3136 beads confined in the square box of length 60 (in units of bead diameter) with the periodic boundary condition. Starting from a well mixed initial state, the snapshots were taken at the moments 0, 15, 30, 50, 80, and 90, which show the evolution of segregation.

PS, the species-dependent interactions were turned on and finally caused the separation. The effective repulsive interaction between A and B will push them apart, and the domains which are rich in A or B grow continuously, until their boundary shrinks to a minimum and a full segregation appears (see the right inset of Fig. 6). For parameters where PS is not allowed, the full segregation is impossible and beads remain in a homogeneous mixed state, depicted in the bottom inset of Fig. 6.

The pattern formation of this segregation is very similar to the well-studied problem of "phase-ordering dynamics" in the nonequilibrium statistical mechanics which refers to a two-phase mixture that evolves out of the homogeneous phase when quenched below the critical coexistence temperature [12,13]. The order parameter, defined as the local difference in densities between the two segregating species, is a function of position and time, which is normalized to between −1 to +1 with each limit corresponding to either the A- or B-rich phase. It is generally accepted that the coarsening domains are characterized by a unique, time-dependent length scale which is approximately equal to the average

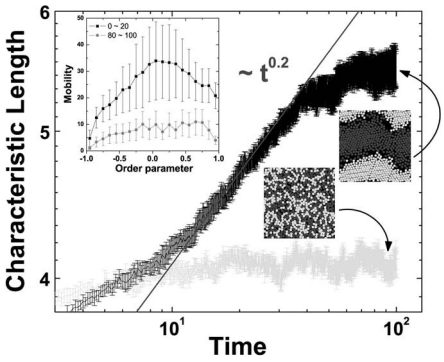

FIG. 6. Time evolution of the characteristic length scale for segregated (in black, $\Gamma=0.1$) and mixed states (in gray, $\Gamma=0.25$) accompanied by their spatial distributions with $f=50$. Error bars are deduced from over ten different initial conditions. The black (gray) data in the left inset show the mobility versus the order parameter in the early (late) stage of the segregation.

thickness of the coarsening domain. We project the whole system onto the x-y plane and calculate the projected two-dimensional order parameter and deduce the characteristic length. Figure 6 shows two typical evolutions of the characteristic length where the black (gray) bars correspond to the segregated (mixed) cases. The power-law exponents range between 1/20 and 1/4 for various parameters. Different from the famous exponents such as 1/2 in Lifshitz-Cahn-Allen growth [12] or 1/3 of Lifshitz-Slyozov growth [12], some features in our system could be identified as follows. (1) The left inset of Fig. 6 shows the mobility (defined as the average horizontal kinetic energy) versus the order parameter in the segregated case, with the black (gray) data points representing the early (late) stage of the segregation. The high mobility near the zero order parameter is a consequence of A-B collisions being out of phase. (2) Furthermore, since the A-B collisions become less frequent as the characteristic length grows during the segregation, the mobility decreases from the black curve to the gray one in the left inset. (3) The most significant difference from the thermodynamic phase separation is the species-dependent mobility, which can be understood by the asymmetric energy dissipation of the A-B and B-B collisions.

The synchronized trajectories of beads A (black line) and B (gray line) are plotted in Fig. 2, where T_1 (T_2) denotes the ascending (descending) time for bead $A$and ϕ_1 (ϕ_2) the phase of the bottom (top) plate at the instant of collision with bead A with the vertical velocity V_n (V_{n+1}). Obviously, PS requires that (i) the velocity after each period has to resume the value of V_n, (ii) the vertical displacement for ascent must exactly cancel that of descent, and (iii) the magnitude of this displacement equals the difference in altitude between ϕ_1 and ϕ_2. These three conditions can be expressed as the following three equations, respectively:

$$\begin{aligned}(1-\epsilon_A^2)V_n &= (1-\epsilon_A)\Gamma\omega C_2 - \epsilon_A(1+\epsilon_A)\Gamma\omega C_1 + \epsilon_A g T_1 - g T_2 \\ &\quad \times[(1+\epsilon_A)\Gamma\omega(C_1-\epsilon_A C_2)+\epsilon_A^2 V_n + \epsilon_A g T_1]T_2 \\ &= \frac{g}{2}(T_1^2+T_2^2) - [(1+\epsilon_A)\Gamma\omega C_1 - \epsilon_A V_n]T_1 \\ &\quad \times[(1+\epsilon_A)\Gamma\omega C_1 - \epsilon_A V_n]T_1 - \frac{g}{2}T_1^2 \\ &= H + \Gamma(S_2 - S_1),\end{aligned}$$

where $T_1+T_2=T$, and $C_{1,2}$ and $S_{1,2}$ correspond to $\cos(\phi_{1,2})$ and $\sin(\phi_{1,2})$. Furthermore, the following constraints must also be fulfilled: $V_n<0$, $V_{n+1}-A\omega\cos(\phi_2)>0$, and the bead cannot fall outside the plates at all times. These conditions determine the valid range of parameters Γ, f, H, and ϵ_A for synchronized trajectories. However, stability analysis has to be checked to guarantee the existence or uniqueness of the solution (ϕ_1,ϕ_2,V_n). The evolution of perturbations dV and $d\phi$ to V_n and ϕ_1 after one period is governed by

$$\begin{pmatrix} dV' \\ d\phi' \end{pmatrix} = D \begin{pmatrix} dV \\ d\phi \end{pmatrix}.$$

The elements of matrix D can be determined by performing the linear stability analysis. This is done by Tayler expanding

the trajectories of both plates to the second order at ϕ_1 and ϕ_2. Afterward, we trace the evolution of the perturbations dV and $d\phi$ analytically via the equation of motion for a bead under the gravity. After doing the calculations, the elements of matrix D are obtained as

$$D_{22} = \frac{1}{\Gamma\omega C_1 - V_n}\{-\epsilon_A[g - (1+\epsilon_A)\Gamma\omega^2 S_1]T_2 + (\Gamma\omega C_2 - V_n)\beta + \beta[\epsilon_A g - (1+\epsilon_A)\Gamma\omega^2 S_2]T_2\},$$

$$D_{21} = \frac{2\pi}{T}\frac{\epsilon_A}{\Gamma\omega C_1 - V_n}\left[\epsilon_A T_2 - \frac{\Gamma\omega C_2 - V_n}{\Gamma\omega C_2 - V_{n+1}}T_1 - \frac{\epsilon_A g - (1+\epsilon_A)\Gamma\omega^2 S_2}{\Gamma\omega C_2 - V_n + 1}T_1 T_2\right],$$

$$D_{11} = \epsilon_A^2 - gD_{21} - \frac{(1+\epsilon_A)(g - \Gamma\omega^2 S_2)}{\Gamma\omega C_2 - V_{n+1}}\epsilon_A T_1,$$

$$D_{12} = \frac{2\pi}{T}\{(1+\epsilon_A)(g - \Gamma\omega^2 S_2)\beta - \epsilon_A[g - (1+\epsilon_A)\Gamma\omega^2 S_1] - gD_{22}\},$$

where β is defined as

$$\beta = \frac{\Gamma\omega C_1 - V_{n+1} - (1+\epsilon_A)\Gamma\omega^2 S_1 T_1}{\Gamma\omega C_2 - V_{n+1}}.$$

The solution is stable if and only if both eigenvalues of D have an absolute magnitude smaller than unity. In general, PS exists for moderate Γ and sufficiently large f. Further increase in Γ first leads to bifurcation where two stable trajectories coexist, and then more and more stable solutions appear before the motion eventually becomes chaotic. Note that we only analyze $n=1$ because simulations reveal that the stable $n>1$ trajectories only exist in the large Γ and nearly elastic regime [10].

In Fig. 7, we present the phase diagram for the segregated and mixed states in the Γ-f plane by simulation. The dark region characterizes PS for all beads. In contrast, only beads A are in PS, while B suffers from bifurcation, in the light gray region. When Γ is not large, the presence of beads A helps B pick out one of the attractors and become effectively PS.

In the limit $\Gamma\omega^2 \gg g$, an extra symmetry $T_1 = T_2$ greatly simplifies the above equations. Analytic solutions become possible, which determine the window for PS as $\Gamma_{\min,(\epsilon_A)} < \Gamma < \Gamma_{\max,(\epsilon_A)}$ where

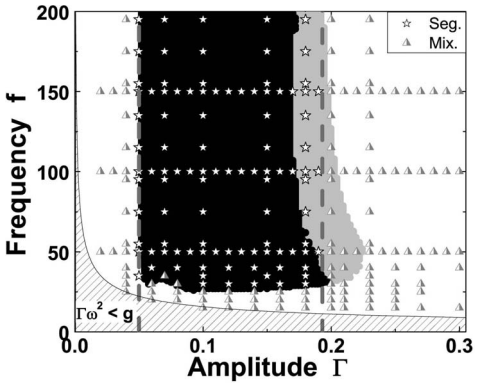

FIG. 7. The stars (triangles) denote the segregated (mixed) state by the simulations. All beads are maintained in PS in the dark region, while beads B experience bifurcation in the gray area. As described in the text, the collisions of beads may help drive B toward one of its two attractors. When this happens, segregation can still happen.

$$\Gamma_{\min,(\epsilon_A)} = \frac{H}{2\sqrt{1+\sigma_A^2}},$$

$$\Gamma_{\max,(\epsilon_A)} = \frac{H\sqrt{16\sigma_A^2 + \pi^4}}{2\sigma_A(\pi^2 - 4)},$$

where $2\sigma_A = \pi(1+\epsilon_A)/(1-\epsilon_A)$. Similar treatments for B give us a second window for B. The overlap between these two guarantees segregation and refers to the upper black region in Fig. 7. The part of the gray region where beads B are forced out of bifurcation and become effectively PS refers to $\Gamma_{\max,(\epsilon_B)} < \Gamma < \Gamma_{\max,(\epsilon_A)}$. We mark the segregation region consisting of these two windows by the dashed lines in Fig. 7, which again is in good agreement with the simulation when $\Gamma\omega^2 \gg g$.

In summary, we have performed both simulations and analytic analysis to confirm the existence of an alternative segregation mechanism. The subject of our study is a nonequilibrium system consisting of two species of beads confined between two vibrating plates. When the motion of beads is in harmony with that of the plates, we observe that segregation can be induced by the phase synchronization of beads. It creates an effective repulsion (attraction) between different (same) species of beads. We believe this phenomenon is general in systems whenever the same (different) species become in (out of) phase.

We acknowledge useful discussions with Professor C. K. Chan, Professor Peilong Chen, Professor P. K. Lai, and Professor K. W. Tu. Support from NSC Grants No. 95-2120-M007-008 and No. 96-2815-C007-006 is acknowledged.

[1] Meiying Hou, Hongen Tu, Rui Liu, Yinchang Li, Kunquan Lu, Pik-Yin Lai, and C. K. Chan, Phys. Rev. Lett. **100**, 068001 (2008).

[2] T. Pöschel and N. Brilliantov, *Granular Gas Dynamics* (Springer, New York, 2003).

[3] Matthias E. Möbius, Benjamin E. Lauderdale, Sidney R. Nagel, and Heinrich M. Jaeger, Nature (London) **414**, 270 (2001); T. Mullin, Phys. Rev. Lett. **84**, 4741 (2000); A. P. J. Breu, H.-M. Ensner, C. A. Kruelle, and I. Rehberg, *ibid.* **90**, 014302 (2003); T. Schnautz, R. Brito, C. A. Kruelle, and I. Rehberg, *ibid.* **95**, 028001 (2005); O. Zik, Dov Levine, S. G. Lipson, S. Shtrikman, and J. Stavans, *ibid.* **73**, 644 (1994).

[4] Paul Melby, Alexis Prevost, David A. Egolf, and Jeffrey S. Urbach, Phys. Rev. E **76**, 051307 (2007).

[5] Matthias Schroter, Stephan Ulrich, Jennifer Kreft, Jack B. Swift, and Harry L. Swinney, Phys. Rev. E **74**, 011307 (2006).

[6] J. B. Knight, H. M. Jaeger, and S. R. Nagel, Phys. Rev. Lett. **70**, 3728 (1993).

[7] N. Burtally, P. J. King, and M. R. Swift, Science **295**, 1877 (2002).

[8] Massimo Pica Ciamarra, Antonio Coniglio, and Mario Nicodemi, Phys. Rev. Lett. **97**, 038001 (2006); M. Tarzia, A. Fierro, M. Nicodemi, M. P. Ciamarra, and A. Coniglio, *ibid.* **95**, 078001 (2005).

[9] This is a standard practice in computer simulations. See, for instance, J. S. van Zon and F. C. MacKintosh, Phys. Rev. E **72**, 051301 (2005).

[10] Edson D. Leonel and P. V. E. McClintock, J. Phys. A **38**, 823 (2005); Denis G. Ladeira and Edson D. Leonel, Chaos **17**, 013119 (2007).

[11] J. M. Luck and Anita Mehta, Phys. Rev. E **48**, 3988 (1993).

[12] J. D. Gunton, M. San Miguel, and P. S. Sahni, in *Phase Transitions and Critical Phenomena*, edited by C. Domb and J. L. Lebowitz (Academic, New York, 1983).

[13] Sanjay Puri, Alan J. Bray, and Joel L. Lebowitz, Phys. Rev. E **56**, 758 (1997).